Supporting information

Atomic Steps Effect on Porous ZnO Nanobelts: Promoting Acetone Gas Detection up to Parts per Trillion-Level

Kyusung Kim, Pil gyu Choi, Toshio Itoh, Yoshitake Masuda*

National Institute of Advanced Industrial Science and Technology (AIST), 2266-98

Anagahora, Shimoshidami, Moriyama, Nagoya 463-8560, Japan

Corresponding author: masuda-y@aist.go.jp (Yoshitake Masuda)

KEYWORDS: ZnO, Nanobelt, Atomic step, Gas sensor

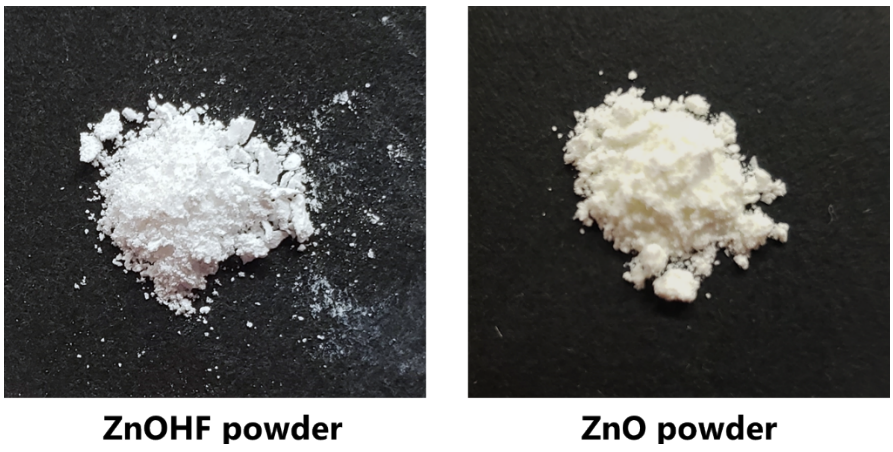

Figure S1. Prepared ZnOHF powder (left side, white) and ZnO powder (right side, light yellow)

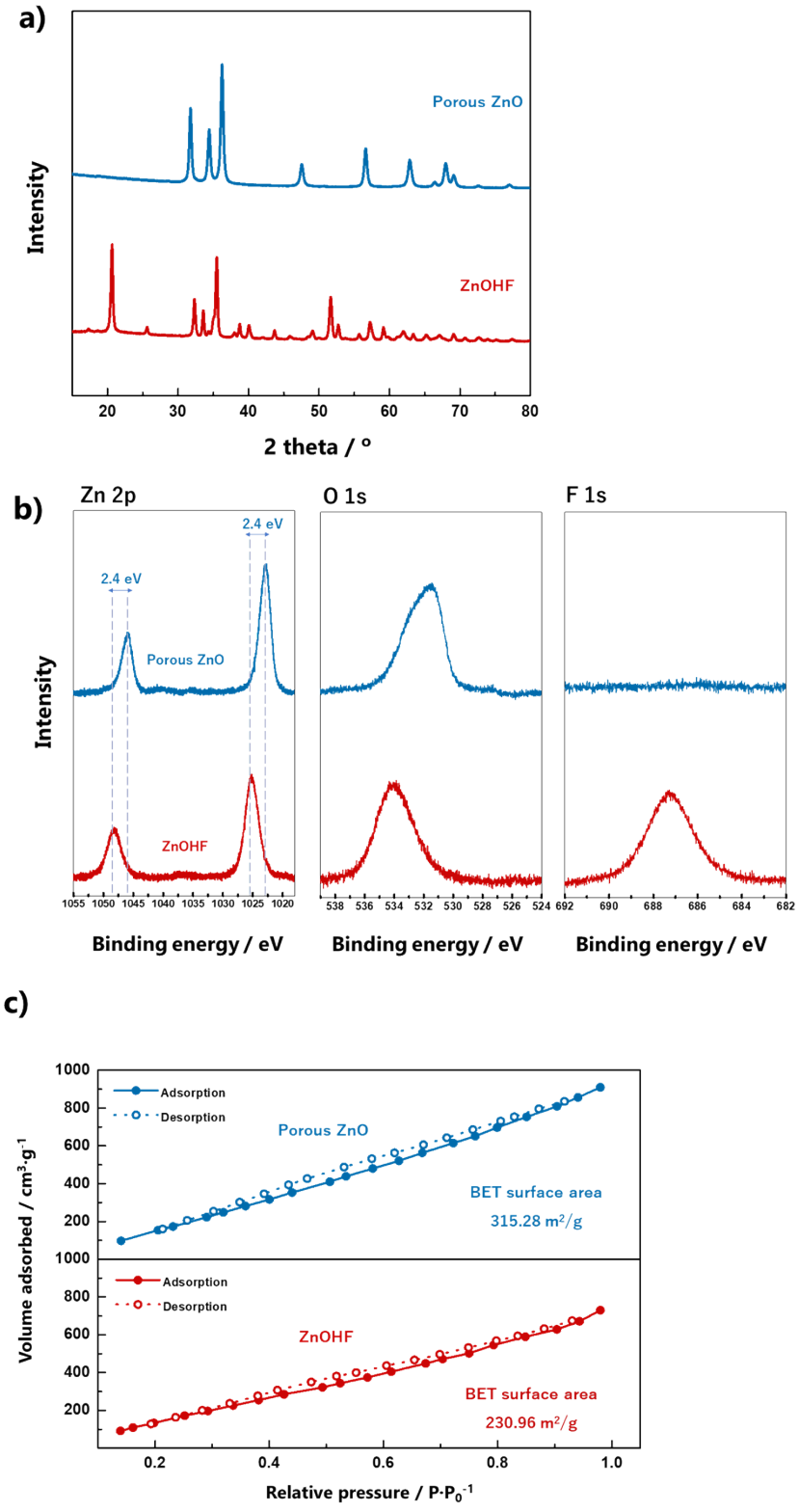

Figure S2. Comparison of a) XRD patterns, b) High-resolution XPS spectra of Zn2p, O1s, and F1s, and c) specific surface area of the porous ZnO and ZnOHF nanobelts.

Table S1 Binding energy and area proportion of deconvoluted peaks in O1s spectra for porous ZnO nanobelt

	Porous ZnO		
	O_L	O_V	O_C
Binding energy [eV]	531.11	532.13	533.03
Area proportion [%]	42.01	28.61	29.37

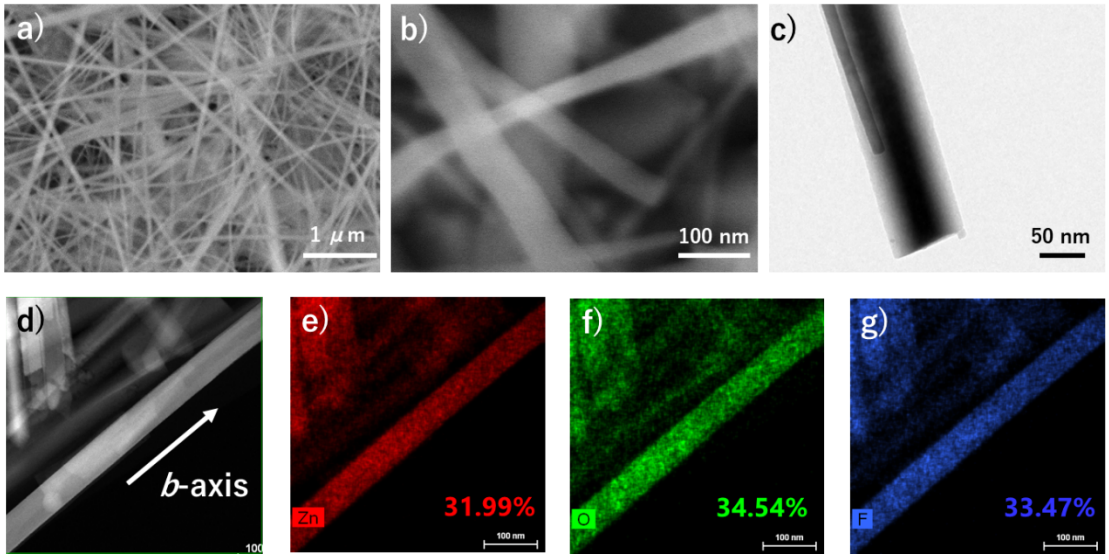

Figure S3 a) Low and b) high magnification SEM images, c) TEM image, d) HAADF-STEM image, and elemental mapping images for e) Zn, f) O, and g) F of the ZnOHF nanobelts.

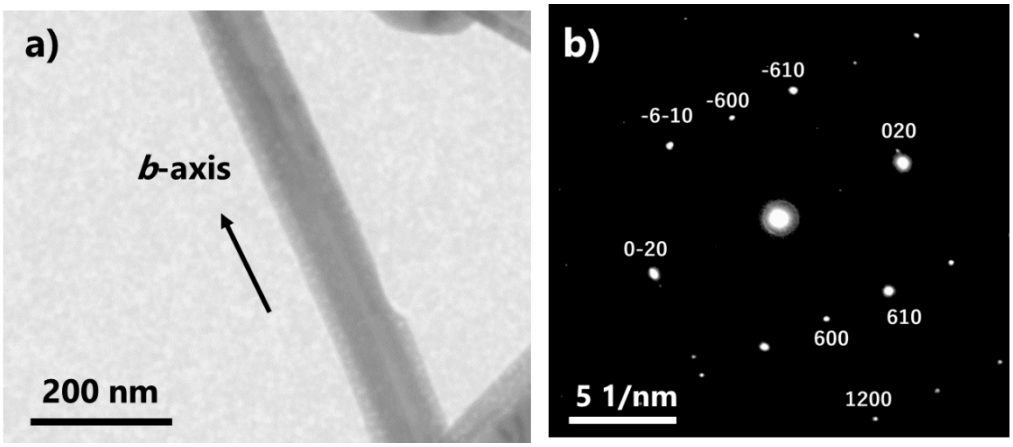

Figure S4 a) Bright-field TEM image and b) SAED pattern of ZnOHF.

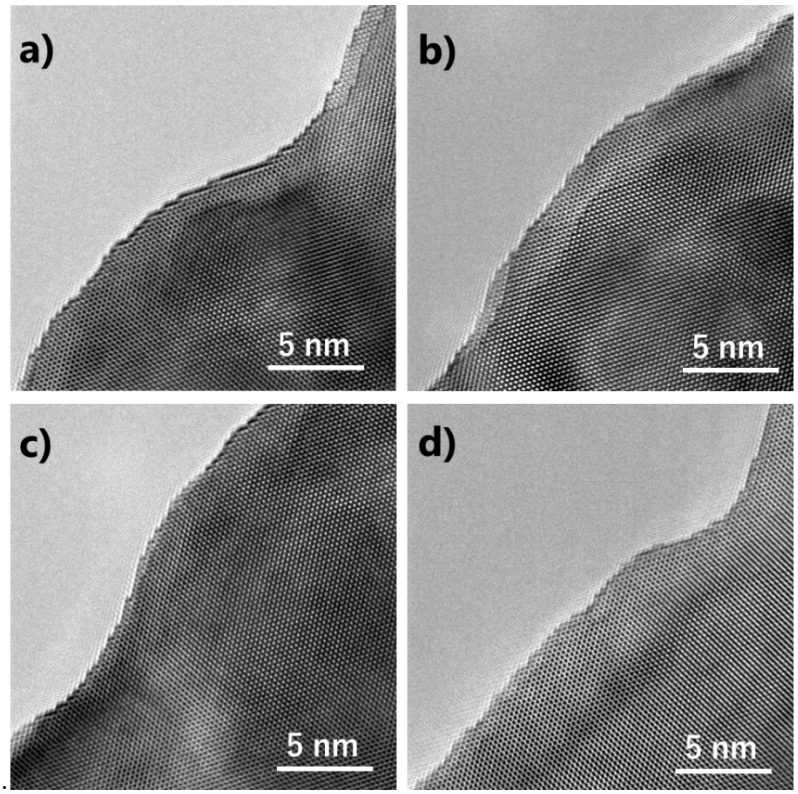

Figure S5 HRTEM images of atomic-step structures on the different positions of the surface.

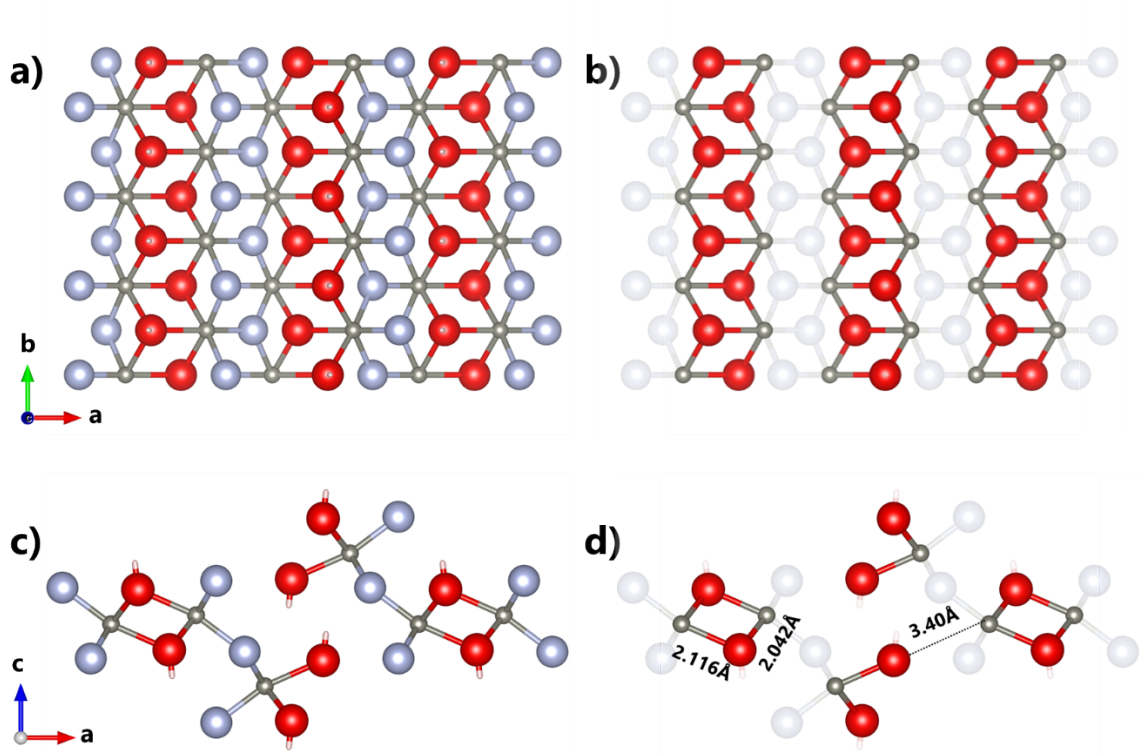

Figure S6 a) projection on the ab plane of typical ZnOHF, b) projection on the ab plane of ZnOHF without H and F, c) projection on the ac plane of typical ZnOHF, and d) projection on the ac plane of ZnOHF without H and F.

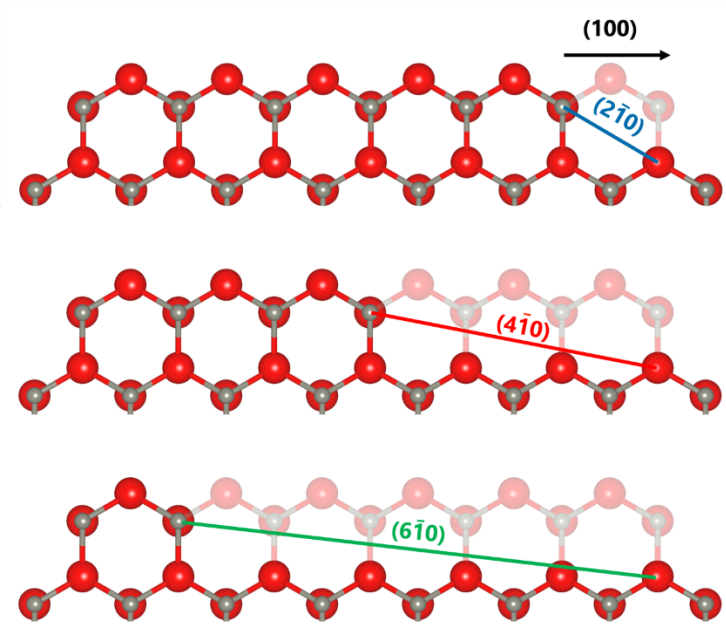

Figure S7 Formation of various types of exposed crystal facets due to atomic-step structure depending on the terrace length.

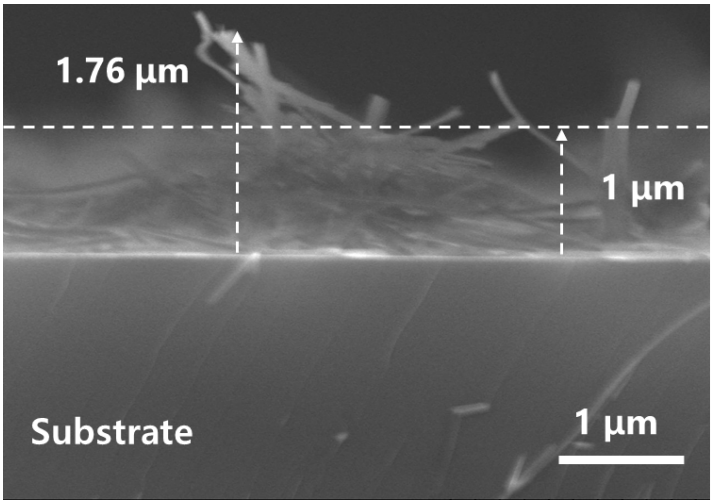

Figure S8. Cross-section of SEM image of the porous ZnO nanobelt film

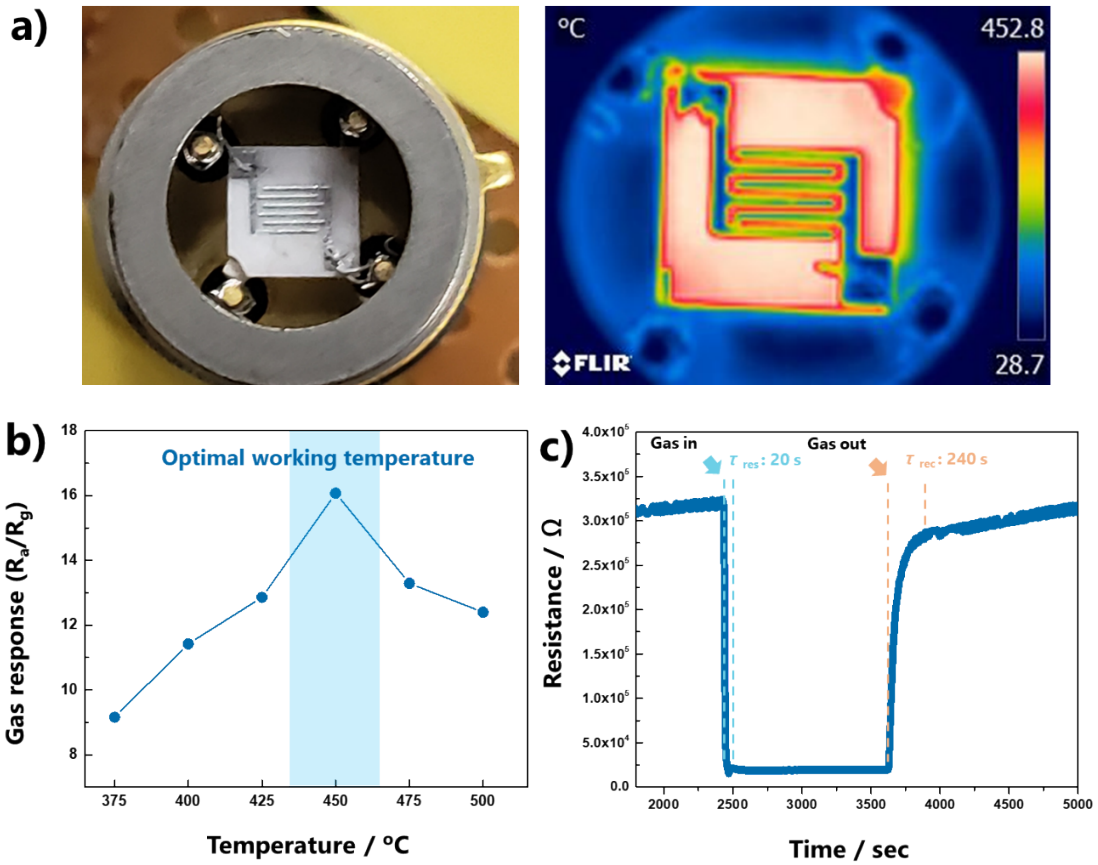

Figure S9 a) photo and thermal distribution images of gas sensor, b) gas response with various operating temperature, and c) response and recovery time of the porous ZnO nanobelt gas sensor at 500 ppb of acetone

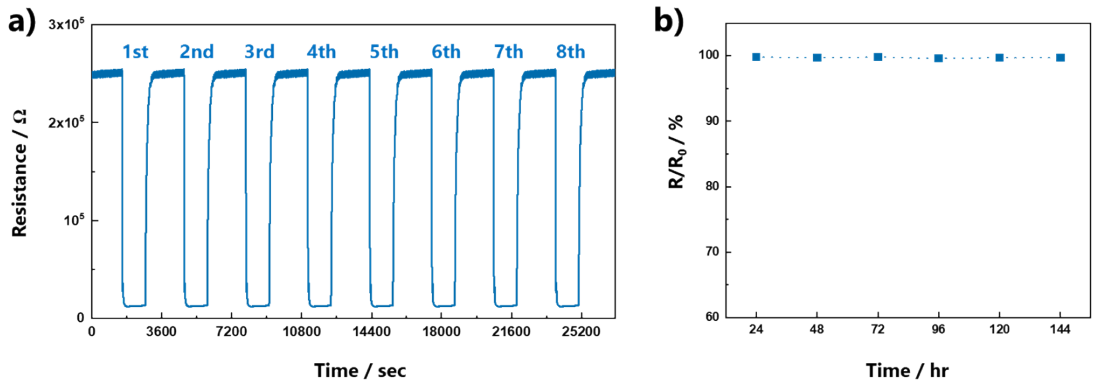

Figure S10. a) Response dynamic curve of ZnO nanobelt sensor upon exposure 500 ppb of acetone for 8 cycles b) ratio between gas response value (R) to initial gas response value (R_0) according to time indicating the stability and repeatability

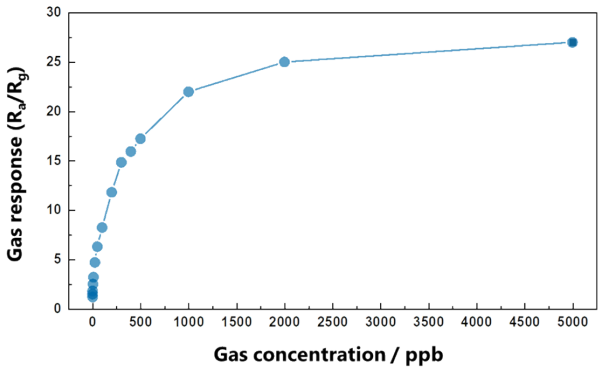

Figure S11 Gas response of porous ZnO nanobelt sensor from ppt range to ppm range.

Table S2 Comparison of gas response and experimental/theoretical LOD of various acetone gas sensors under ppb level.

Material	Conc. [ppb]	Gas response	Experimental /Theoretical LOD [ppb]	Ref.
Porous ZnO nanobelt	**500**	**15.98**	**0.2 / 0.072**	**This work**
Ag-CuO/Cu_2O nanopattern	500	10.6	125 / -	[32]
Au/In_2O_3 3D film	500	10	20 / 15	[33]
Pt-In_2O_3 nanofiber	300	10.2	10 / -	[34]
ZnO−CuO hollow cube	500	5.59	40 / 9	[35]
Rh_2O_3-WO_3 nanofibers	1000	11.9	1000 / 100	[36]
SnO_2 nanosheet	400	5.6	200 / 110	[37]
PdAu-SnO2	500	2.5	100 / 45	[38]
Ru-WO_3 nanorod	400	6.8	200 / 0.131	[39]
WO_3 nanowire	1000	6.1	1000 / 2	[40]
$W_{18}O_{49}$/Ti_3C_2Tx	500	1.8	170 / -	[41]
ZnO/MoS_2 nanosheets	500	2.86	5/-	[42]
ZnO/MoS_2 core/shell	500	2.5	100/-	[43]

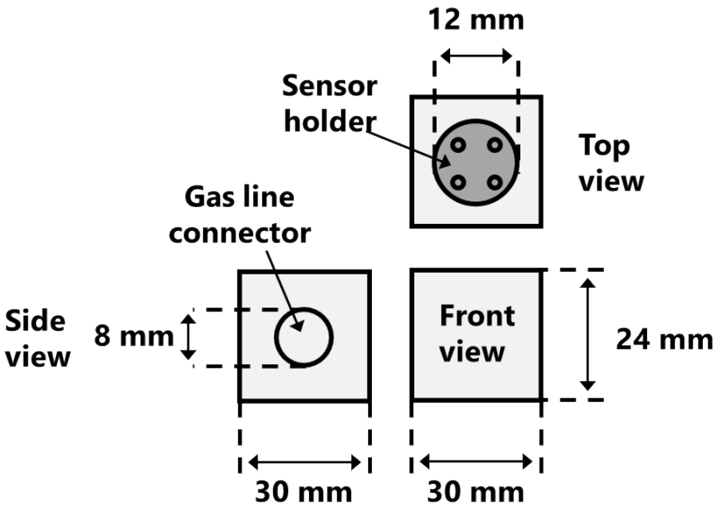

Figure S12 Top, side and front view of gas sensing chamber.